

## Organic-inorganic hybrid zeolite silica materials by grafting of trimethylchlorosilane TMCS: part I: preparation and characterization

O. Bouchher<sup>1</sup>, K. Benrachedi<sup>1</sup>, M. Makhoulouf<sup>2</sup>, S. M. Messabih<sup>1</sup>, K. Louhab<sup>1</sup>

<sup>1</sup>Food Technology Research Laboratory (LRTA) Faculty of Sciences Engineer  
University of M'hamed Bougara, Boumerdes, 35000 Boumerdes–Algeria

<sup>2</sup>Military Academy of Cherchell-Defunt President Houari Boumedie-Tipaza-Algeria

\*Corresponding author: o.bouchher@univ-boumerdes.dz; Tel.: +213 00 00 00; Fax: +21300 00 00

### ARTICLE INFO

#### Article History :

Received : 03/07/2018

Accepted : 28/05/2020

#### Key Words:

Zeolite X;  
Grafting;  
TMCS;  
Functionalization.

### ABSTRACT/RESUME

**Abstract:** The functionalization of our 13X zeolite was carried out by the post-synthesis method using an organosilane of the Trimethylchlorosilane type (TMCS) to obtain a more hydrophobic organic-inorganic hybrid zeolite. Our zeolite before and after grafting was characterized by different analysis techniques (XRD, FTIR, BET, and SEM). The XRD results of the grafted 13X zeolite, show that the functionalization does not destroy the crystal structure of the material. FT-IR analysis of the 13X zeolite before and after grafting confirms the grafting of our organosilane on the surface by the disappearance of the absorption band of the silanol groups at 980  $\text{cm}^{-1}$  and the appearance of a band of absorption attributed to the vibrations of the trimethylsilyl Si ( $\text{CH}_3$ ) group at 2970  $\text{cm}^{-1}$ . The specific surface area of our grafted 13X has been reduced by 63.22  $\text{m}^2 / \text{g}$  thanks to the organic group which has been grafted on the external surface. According to SEM results, the morphology of the surface of our material was slightly modified after grafting. The results of various analyses demonstrated that the grafted 13X zeolite is successfully obtained using the post-synthesis method.

### I. Introduction

Porous sorbents such as zeolites, porous silicas, activated carbons, have widespread applications in the field of purification processes and catalysis. Zeolites, among all types of porous materials, possess the best technological impact due to their variety, their stability, their catalytic activity and their behavior as selective adsorbents and ion exchangers. These physicochemical properties of zeolites explain the interest of scientific research on these materials to widen their field of application. Zeolites are naturally occurring clay-like compounds that come from volcanic earth deposits produced from the interaction between ash and volcanic rock with underground water. Their porous nature has been crystallized and developed over a long period of time in lake and marine basins [1].

Zeolites are crystalline aluminosilicates of alkali and alkaline earth elements such as sodium, potassium and calcium. Their empirical formula is  $\text{M}_{n/2}\text{O}[(\text{Al}_2\text{O}_3)(\text{SiO}_2)_x]y\text{H}_2\text{O}$  where x varies between 2 and 10, n is the cation valence, and y represents the water contained in their pores [2, 3]. The crystal lattice consists of the three-dimensional arrangement of tetrahedron ( $\text{SiO}_4$ ) and ( $\text{AlO}_4$ ) - linked by their vertices. These sequences form polyhedra which are arranged in a given symmetry to form the crystal. The vacant space delimited by the aluminosilicate framework is organized in a network of cavities connected by pores of uniform size (effective pore diameter from 3 to 10 Å) [4]. The cations M and the water molecules constitute extra-structural spaces. The cations compensate the negative charges induced by the aluminum atoms of the framework and can be exchanged to adjust the adsorption properties. The water occupying the

pores can be desorbed by heating under vacuum or sweeping dry gas [4, 5].

Natural zeolites are more than 40 types [6]; they are used as filtering agents and molecular sieves to remove various pollutants and heavy metals from the atmosphere, earth and water.

Synthetic zeolites, prepared in the laboratory, are more efficient and more used than natural zeolites because of their high adsorption capacity and their selectivity [7].

In general, zeolites are good acidic catalysts [8]. This acidity is due to the presence of different types of acid sites such as Bronsted acid sites which are hydroxyl groups (-OH) [9] located at the same time, inside the pores and on the outer surface of the zeolites.

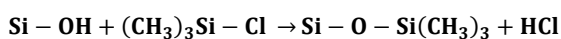
These hydroxyl groups can be reacted with an organosilane to give a hybrid material [10].

Hybrid materials are obtained by the functionalization of zeolite materials by an organic compound using the post-synthesis method which is widely used in this type of synthesis [11 - 13].

## II. Materials and methods

### II.1. Sample preparation and functionalization

The zeolite X used in this study is a commercial synthetic zeolite (Aldrich). The chemical modification of this material is carried out using the post-synthesis technique. This technique is based on substitution reactions between the silanol (Si-OH) groups of the surface and an organosilane of the type (TMCS) according to the following reaction:



Before the silylation reaction, the material should be calcined under air at a temperature of 550 °C for 12 hours to remove the structuring agent and open the pores.

The functionalization method used in this study is that described by X.S.Zhao et al [14]. In this method, 2 g of our zeolite is introduced into a vacuum oven at a temperature of 250-300 °C for 4 hours to remove the water molecules that are inside the pores. After degassing, the material is directly added to a refluxing solution of TMCS in toluene at a mass concentration of 5% with the proportion (1g: 50ml) at a temperature of 70 °C for 3h. After filtration, the mixture is washed by toluene and then by acetone to remove chemical residues. Finally, our hybrid materials are filtered and dried in an oven at 80 °C.

### II.2. Physicochemical characterization

The nitrogen adsorption-desorption isotherms of the studied materials were obtained at a temperature of

77 K using a NOVA 1200 analyzer. The specific surface and the pore volume of our studied samples were calculated using the BET method. The morphology of the surface of the 13X zeolite before and after grafting was observed by an EVO MA 25 scanning electron microscope (Carl Zeiss Microscopy Limited). An infrared spectrometer of the Perkin-Elmer 2000 type was used to confirm the chemical modification of the surface of our materials before and after grafting in a spectral range from 400cm<sup>-1</sup> to 4000cm<sup>-1</sup>. The diffractograms of the materials studied were obtained at the same time using a CuK $\alpha$  radiation diffractometer of the Bruker D8 Advanced X-ray type.

## III. Results and discussion

### III.1. X-Ray Diffraction (XRD)

The diffractograms of our materials, 13X and 13X graft (13X-G), are shown in Fig. 1 and Fig.2. These diffractograms show the presence of the characteristic reflections of the 13X zeolite.

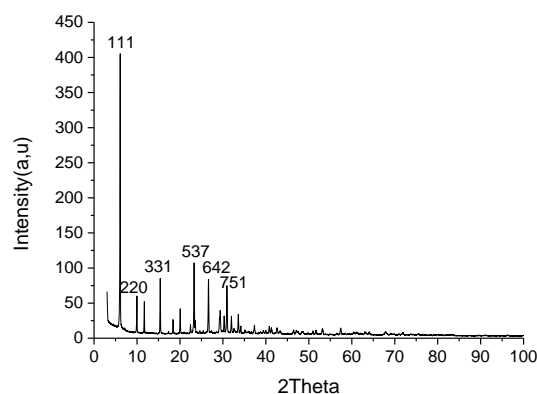


**Figure 1.** XRD pattern recorded on calcined 13X

By comparing the diffractograms of 13X zeolite before and after grafting, slight differences in the peaks are observed, the decrease of the intensity of the intense peaks (111), which indicates the replacement of the silanol groups (Si-OH) by organic groups. This confirms that the crystalline structure of our material is maintained after functionalization.

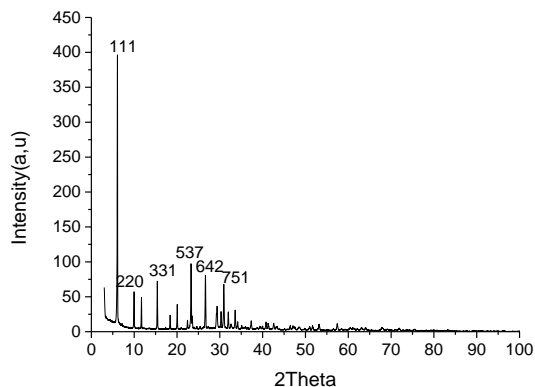


Figure 2. XRD pattern recorded on grafted 13X

### III.2. Fourier Transform Infra-Red (FT-IR)

The FT-IR spectra of 13X zeolite before and after grafting were recorded in the 4000-400  $\text{cm}^{-1}$  range. These spectra (Fig.3 and Fig.4) show the appearance and disappearance of various absorption bands after grafting. The FT-IR spectra (fig.3 and fig.4) of our materials show the absorption band at 462  $\text{cm}^{-1}$  corresponding to the T- O (T = Si or Al) bending vibration of the  $\text{SiO}_4$  and  $\text{AlO}_4$  internal tetrahedra. Peaks at 672  $\text{cm}^{-1}$  (Fig. 3) and 641  $\text{cm}^{-1}$  (Fig. 4) corresponding to the symmetric stretching vibration of the internal tetrahedra [15] and peaks observed at 1638  $\text{cm}^{-1}$  (Fig.3) and at 1620  $\text{cm}^{-1}$  (Fig.4) which are attributed to the H-O-H bending vibration of water molecule [16].

The FT-IR spectra of the calcined 13X zeolite show the main bands, two of which are large and very intense, the first peak at about 980  $\text{cm}^{-1}$  is attributed to the symmetrical stretching vibration of the silanol Si-OH groups [17]. While the second peak at about 3472  $\text{cm}^{-1}$  is assigned to the O-H stretching vibration of the water molecules that are absorbed in the zeolite cavities and channels [18]. Peaks observed at 566  $\text{cm}^{-1}$  and 754  $\text{cm}^{-1}$  and corresponding respectively to the vibration of the double six member rings and the symmetrical stretching vibration of the external linkage [19,20]. The weak band at 1388-1490  $\text{cm}^{-1}$  may be affected by the excess alumina in the pores [21]

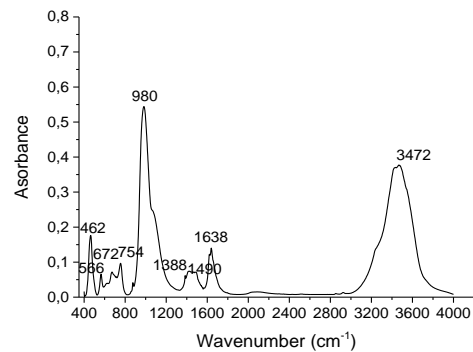


Figure 3. FTIR spectrum of calcined 13X zeolite

On the other hand, The FT-IR spectra of grafted 13X zeolite shows the disappearance of the band 980  $\text{cm}^{-1}$ , this spectrum also shows the appearance of four additional bands, one of which is wide and very intense, the first band around 1074  $\text{cm}^{-1}$  corresponding to the Si-O-Si stretching vibration, the second band around 800  $\text{cm}^{-1}$  corresponding to the Si-O-Si bending vibration [22], the third band at 952  $\text{cm}^{-1}$  asymmetrical stretching vibration of the internal tetrahedra  $\text{TO}_4$  and the fourth band around 2962  $\text{cm}^{-1}$  is attributed to the stretching vibration of the Trimethylsilyl Si-( $\text{CH}_3$ ) group obtained after the functionalization of the 13X zeolite [13]. The disappearance of the band at 980  $\text{cm}^{-1}$  and the appearance of a new band at 2962  $\text{cm}^{-1}$  is explained by the replacement of the silanol groups (Si-OH) by the Trimethylsilyl groups Si( $\text{CH}_3$ ) and confirms the functionalization of our material.

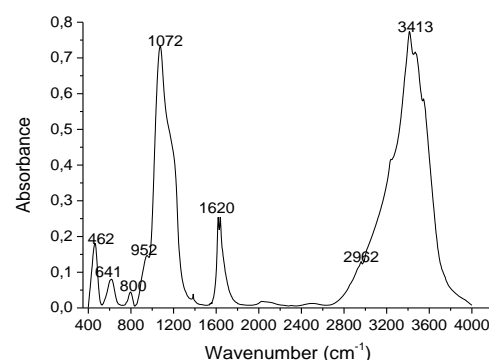
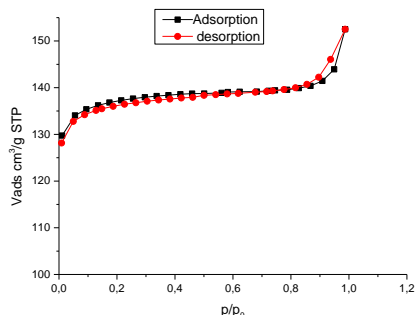


Figure 4. FTIR spectrum of grafted 13X zeolite

### III.3. Nitrogen adsorption-desorption isotherm (BET analysis)

The nitrogen adsorption-desorption isotherms of calcined 13X zeolite are shown in Fig.5. It is found

that the isotherms of our material are types I which is a characteristic of microporous materials (according to the IUPAC recommendation) [23].



**Figure 5.** Nitrogen adsorption – desorption isotherms of calcined 13X zeolite

Fig. 5 shows that the adsorption-desorption curves of N<sub>2</sub> in the 13X zeolite before grafting are superposable. The adsorption of the nitrogen molecules is at the same relative pressures as the desorption. For low pressures, the adsorption isotherm results in the appearance of a liquid nitrogen film on the surface of the pores to form the mono-multilayers. A final plateau with a small inclination at high relative pressures, corresponding to the adsorption on the external surface of our material.

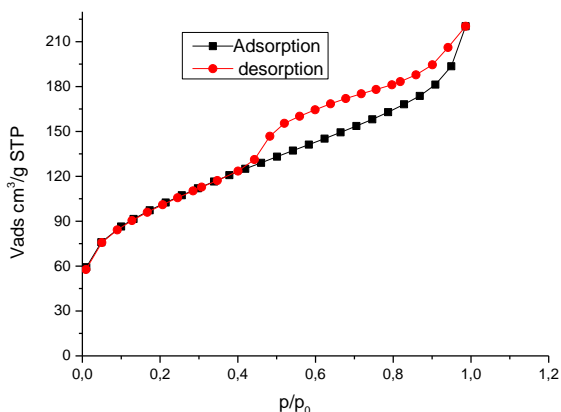


**Figure 6.** Nitrogen adsorption – desorption isotherms of grafted 13X zeolite

The N<sub>2</sub> adsorption-desorption isotherms of the grafted 13X zeolite (13X-G) are not superposable in comparison with the calcined 13X zeolite. As seen from Fig.6, the N<sub>2</sub> adsorption-desorption isotherms of our material exhibit both type I and IV isotherms, corresponding to hierarchical porosity ranging from micropore to mesopore [24].

The adsorption of nitrogen molecules does not occur at the same relative pressures as desorption. The hysteresis presented in Fig. 6 indicates a phenomenon of capillary condensation in the

pores[25]. These results support a heterogeneous distribution of pore size.

The textural properties determined after exploitation of the nitrogen adsorption-desorption analysis data are shown in Table 1.

**Table 1.** Physical and textural properties of the studied materials

Sample	SBET (m <sup>2</sup> g <sup>-1</sup> )	Vpore (ml.g <sup>-1</sup> )	Dpore (Å)	DBJH (Å)
13X	413.02	0.34	22.84	71.71
13X -G	349.78	0.23	27.80	47,95

In general, there is a decrease in the specific surface, the pore volume, the average diameter BJH after silylation.

The decrease of these parameters is relative to the replacement of the silanol groups (Si-OH) by trimethylsilyl Si (CH<sub>3</sub>) groups of larger size. However, values are still characteristic of microporous solids.

#### III.4. Scanning electron microscope (SEM)

The images shown in Fig.7 and Fig.8, obtained by the scanning electron microscope, show the morphology of the outer surface of the 13X zeolite before and after grafting.

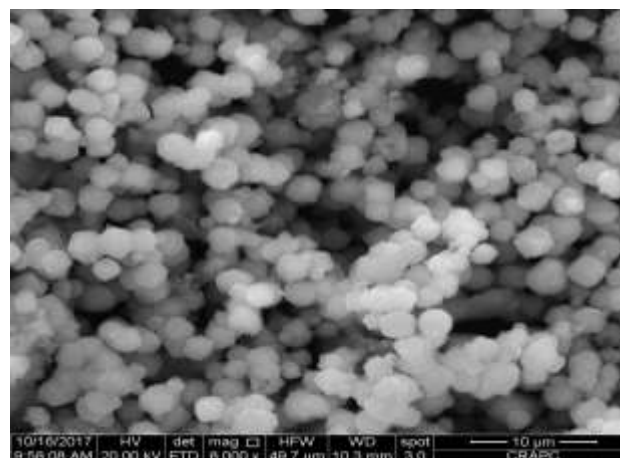


**Figure 7.** SEM micrograph of calcined 13X zeolite

The image of Fig.7 shows the homogeneity of the size of the basic structural unit of the 13X zeolite before grafting. The image of Fig. 8 shows that the size of the basic structural unit of our post-graft material is less homogeneous because of the chemical modification of certain active properties of the surface by the silylation reaction material.

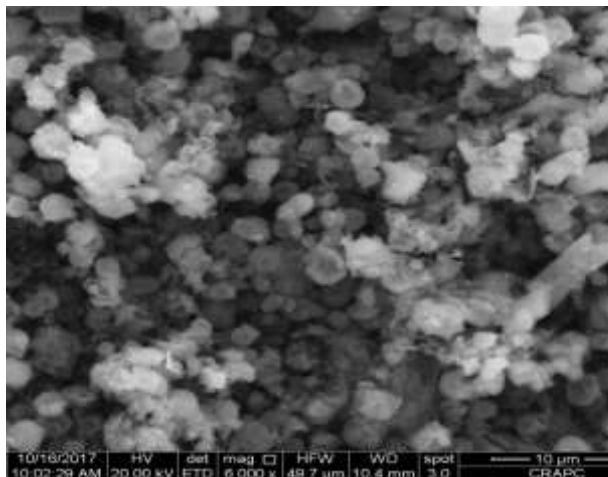


Fig.8. SEM micrograph of grafted 13X zeolite

#### IV. Conclusion

Our synthesized 13X zeolite has been modified to be more hydrophobic by grafting an organosilane of the TMCS type on its surface using the post-synthesis method. The grafting of the trimethylsilyl group was confirmed by FT-IR analyses and by the reduction in the specific surface and the pore volume. According to XRD and SEM results, the crystal structure and the surface morphology of our material after grafting have been maintained. The results of this study show that the grafting method used is very effective because it allows the insertion of organic functional groups, on the surface of our zeolite, by covalent bonds without affecting the crystalline form of the material. Our grafted zeolite can be used for selective and very specific applications in the field of adsorption such as removal of heavy metals, adsorption of organic matter from wastewater and adsorption of CO<sub>2</sub> in water.

#### V. References

- Moshoeshoe, M.; Nadiye-Tabbiruka, M. S.; Obuseng, V. Review of the Chemistry, Structure, Properties and Applications of Zeolites. *American Journal of Materials Science* 7 (5) (2017) 196-221
- Rahman, M. M.; Hasnida, N.; Nik, W. W. Preparation of Zeolite Y Using Local Raw Material Rice Husk as a Silica Source. *Journal of Scientific Research* 1 (2) (2009) 285-291
- Rao, G.P.C.; Satyaveni, S.; Ramesh, A.; Seshaiyah, K.; Murthy, K.S.N.; Choudary, N.V. Sorption of cadmium and zinc from aqueous solutions by zeolite 4A, zeolite 13X and bentonite. *J. Environ. Manage* 81 (2006) 265-272.
- Deer, W. A.; Howie, R. A.; Wise, W. S.; Zussmann, J. Rock-forming minerals Volume 4B. Framework silicates: Silica minerals, Feldspathoids and the Zeolites. *Geological Magazine* 143 (4) (2004) 557-557
- Stocker, K.; Ellersdorfer, M.; Lehner, M.; Raith, J. G. Characterization and Utilization of Natural Zeolites in Technical Applications. *BHM Berg-und Hüttenmännische Monatshefte* 162 (4) (2017) 142-147.
- Hovhannisyanyan, V. A.; Dong, C. Y.; Lai, F. J.; Chang, N. S.; Chen, S. J. Natural zeolite for adsorbing and release of functional materials. *Journal of Biomedical Optics* 23(9) (2018) 091411
- Bennett, G. F.; Yang, R. T. Adsorbents: fundamentals and applications. *Journal of Hazardous Materials*, 1(109) (2004) 227-228.
- Ennaert, T.; Van Aelst, J.; Dijkmans, J.; De Clercq, R.; Schutyser, W.; Dusselier, M.; Sels, B. F. Potential and challenges of zeolite chemistry in the catalytic conversion of biomass. *Chemical Society Reviews* 45 (3) (2016) 584-611
- Zhang, L.; Chen, K.; Chen, B.; White, J. L.; Resasco, D. E. Factors that determine zeolite stability in hot liquid water. *Journal of the American Chemical Society* 137(36) (2015) 11810-11819
- Ratner, B. D.; Hoffman, A. S.; McArthur, S. L. Physicochemical Surface Modification of Materials Used in Medicine. *Biomaterials Science* (2020) 487-505
- Sayari, A.; Hamoudi, S. Periodic mesoporous silica-based organic-inorganic nanocomposite materials. *Chemistry of Materials* 13(10) (2001) 3151-3168
- Shang, F.; Wu, S.; Guan, J.; Sun, J.; Liu, H.; Wang, C.; Kan, Q. A Comparative study of aminopropyl-functionalized SBA-15 prepared by grafting in different solvents. *Reaction Kinetics, Mechanisms and Catalysis* 103(1) (2011) 181-190
- Maria Chong, A. S.; Zhao, X. S. Functionalization of SBA-15 with APTES and characterization of functionalized materials. *The Journal of Physical Chemistry B* 107(46) (2003) 12650-12657.
- Zhao, X. S.; Lu, G. Q. Modification of MCM-41 by Surface Silylation with Trimethylchlorosilane and Adsorption Study. *The Journal of Physical Chemistry B* 102 (9) (1998) 1556-1561
- Byrappa, K.; Suresh Kumar, B.V. Characterization of Zeolite by Infrared Spectroscopy. *Asian Journal of Chemistry* 19 (6) (2007) 4933-4935.
- Ma, Y.; Yan, C.; Alshameri, A.; Qiu, X.; Zhou, C. Synthesis and characterization of 13X zeolite from low-grade natural kaolin. *Advanced Powder Technology* 25 (2) (2014) 495-499
- Zhao, X. S.; Lu, G. Q.; Hu, X. Characterization of the structural and surface properties of chemically modified MCM-41 material. *Microporous and Mesoporous Materials* 41(1-3) (2000) 37 - 47
- Sasikala, S.; Gopi, K. H.; Bhat, S. D. Sulfosuccinic acid-sulfonated polyether ether ketone/organic functionalized microporous zeolite-13X membrane electrolyte for direct methanol fuel cells. *Microporous and Mesoporous Materials* 236 (2016) 38-47.
- Chen, D.; Hu, X.; Shi, L.; Cui, Q.; Wang, H.; Yao, H. Synthesis and characterization of zeolite X from lithium slag. *Applied Clay Science* 59 (2012) 148-151.
- Zhan, B.Z.; White, M.A.; Lumsden, M.; Mueller-Neuhaus, J.; Robertson, K.N.; Cameron, T.S.; Gharghoury, M. Control of Particle Size and Surface Properties of Crystals of NaX Zeolite. *Chemistry of Materials* 14(9) (2002) 3636-3642.
- Byrappa, K.; Kumar, B. S. Characterization of zeolites by infrared spectroscopy. *Asian journal of chemistry* 19(6) (2007) 4933 -4933
- Meléndez-Ortiz, H. I.; Perera-Mercado, Y.; Mercado-Silva, J. A.; Olivares-Maldonado, Y.; Castruita, G.;

- García-Cerda, L. A. Functionalization with amine-containing organosilane of mesoporous silica MCM-41 and MCM-48 obtained at room temperature. *Ceramics International* 40(7) (2014) 9701–9707
23. Rongchapo, W.; Deekamwong, K.; Loiha, S.; Prayoonpokarach, S.; Wittayakun, J. Paraquat adsorption on NaX and Al-MCM-41. *Water Science and Technology* 71(9) (2015) 1347–1353.
24. Cheng, W. P.; Gao, W.; Cui, X.; Ma, J. H.; Li, R. F. Phenol adsorption equilibrium and kinetics on zeolite X/activated carbon composite. *Journal of the Taiwan Institute of Chemical Engineers* 62 (2016) 192-198
25. Barsotti, E.; P. Tan, S.; Saraji, S.; Piri, M.; Chen, J.H. A review on capillary condensation in nanoporous media: Implications for hydrocarbon recovery from tight reservoirs. *Journal homepage, Fuel* 184 (2016) 344 -361

**Please cite this Article as:**

Bouchher O., Benrachedi K., Makhlouf M., Messabih S.M., Louhab K., Organic-Inorganic Hybrid Zeolite Silica Materials by Grafting of Trimethylchlorosilane TMCS: Part I: Preparation and characterization, *Algerian J. Env. Sc. Technology*, 7:2 (2021) 1944-1949